Available online at www.derpharmachemica.com

ISSN 0975-413X
CODEN (USA): PCHHAX

Der Pharma Chemica, 2016, 8(11):1-11
(http://derpharmachemica.com/archive.html)

A quantum chemical analysis of the inhibition of protein kinase A (PKA) and Rho-associated protein kinase-2 (ROCK2) by a series of urea-based molecules

Juan S. Gómez-Jeria* and Massiel Matus-Pérez

Quantum Pharmacology Unit, Department of Chemistry, Faculty of Sciences, University of Chile. Las Palmeras 3425, Santiago 7800003, Chile

---

ABSTRACT

A theoretical analysis of the relationships between electronic structure and the inhibition of ROCK2 and PKA kinases was carried out for a series of urea-based derivatives. The Klopman-Peradejordi-Gómez formal method was used. The local atomic reactivity indices were obtained at the B3LYP/6-31G(d,p) level after full geometry optimization. Statistically significant equations relating several local atomic reactivity indices with both inhibitory activities were obtained. From the results, the corresponding partial 2D pharmacophores were built.

Keywords: ROCK2, PKA, QSAR, urea-based molecules, protein kinase, KPG method.

INTRODUCTION

During the search of molecular systems having interesting biological activities to be studied with the Klopman-Peradejordi-Gómez (KPG) method, we found a series of urea-based derivatives having the ability to inhibit ROCK2 and PKA protein kinases [1]. ROCK2 or rho associated coiled-coil containing protein kinase 2, is a protein regulating the activation of the c-fos serum response element cytokinesis, smooth muscle contraction and the formation of actin stress fibers and focal adhesions [2-7]. Two isoforms, ROCK1 and ROCK2, are known. PKA, cAMP-dependent protein kinase or protein kinase A has numerous functions in the cell, including regulation of lipid metabolism, glycogen and sugar. Many molecular systems inhibiting one or both kinases have been synthesized and tested [1, 8-26]. Here we present the results of a search for relationships between the electronic structure of this series of urea-based molecules and the abovementioned inhibitory activities.

MATERIALS AND METHODS

The method employed here to obtain relationships between the electronic structure and biological activity is the only member of the *formal* methods class [27-29]. It is essentially based on the statistical-mechanical definition of the equilibrium constant and Klopman's formula for the interaction energy between two molecular systems (ΔE) [30, 31]. The first version of this model was employed by Peradejordi et al., Tomás and Aulló and J.S. G.-J. [30, 32-38]. It provided very good results for several different kinds of molecules and receptors. During the 1980 decade the interaction energy expression was expanded to include the contribution of single molecular orbitals [39]. During year 2002 the conceptual basis for calculating the orientational parameter of the substituents was presented [40]. The last theoretical advance was completed during year 2012 when new local atomic reactivity indices were obtained from the ΔE expression [41]. Also, during year 2012 a breakthrough was accomplished when it was shown that the

method can be applied fruitfully to any biological activity [42]. From this moment the application of the Klopman-Peradejordi-Gómez method (KPG) to very different molecules and biological activities produced surprisingly good results [43-52] (and references therein). Considering that the formula has been presented and explained in detail in many publications, we shall discuss here only the resulting equations.

Selection of molecules and biological activities

The selected molecules are a group of urea-based molecules were selected from a recent study [1]. Their general formula and inhibitory activities are displayed, respectively, in Fig. 1 and Table 2.

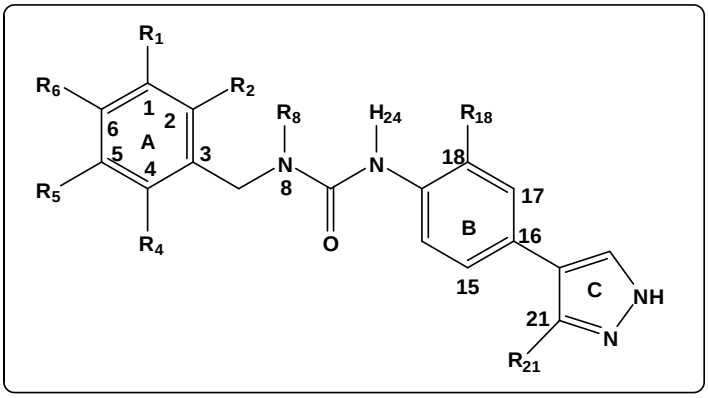

Figure 1. General formula of urea-based molecules

Table 1. Urea-based derivatives and biological activities [1].

Mol.	R_1	R_2	R_4	R_5	R_6	R_8	R_{18}	R_{21}	log(IC_{50}) ROCK2	log(IC_{50}) PKA
1	H	OMe	H	H	H	H	H	H	1.42	2.82
2	H	H	H	H	OMe	H	H	H	3.44	---
3	OMe	H	H	H	H	H	H	H	1.52	3.42
4	NH_2	H	H	H	H	H	H	H	0.48	2.61
5	Cl	H	H	H	H	H	H	H	1.23	2.66
6	F	H	H	H	H	H	H	H	0.48	2.51
7	OMe	H	H	H	H	H	H	Me	0.30	2.91
8	OMe	H	H	H	H	H	$N(Me)_2$	H	---	1.58
9	OMe	H	H	H	H	H	OMe	H	---	2.21
10	OMe	H	H	H	H	H	Cl	H	---	2.50
11	OMe	H	H	H	H	H	F	H	---	3.26
12	OMe	H	H	H	H	H	$O(CH_2)_2N(Me)_2$	H	---	3.59
13	OMe	H	H	H	H	H	$O(CH_2)_2N(CH_2)_4$	H	---	3.44
14	OMe	H	H	H	H	H	$N(Me)\ (CH_2)_2N(Me)_2$	H	---	3.55
15	OMe	H	H	H	H	Me	$O(CH_2)_2N(Me)_2$	H	---	3.72
16	OMe	H	H	H	H	Me	$N(Me)\ (CH_2)_2N(Me)_2$	H	0.90	3.66
17	OMe	H	H	H	H	H	H	H	0.30	2.95
18	OMe	OMe	H	H	H	H	H	H	2.40	---
19	H	OMe	H	H	OMe	H	H	H	2.52	4.05
20	H	OMe	H	OMe	H	H	H	H	2.76	---
21	H	OMe	OMe	H	H	H	H	H	2.97	4.13
22	OMe	H	H	H	OMe	H	H	H	2.63	---
23	OMe	H	H	OMe	H	H	H	H	2.45	---
24	F	H	H	H	OMe	H	H	H	2.55	2.71
25	OMe	H	H	H	H	Me	H	H	0.0	3.26

Calculations

The electronic structure of all molecules was calculated within the Density Functional Theory (DFT) at the B3LYP/6-31g(d,p) level with full geometry optimization. The Gaussian suite of programs was used [53]. All the information needed to calculate numerical values for the local atomic reactivity indices was obtained from the Gaussian results with the D-Cent-QSAR software [54]. All the electron populations smaller than or equal to 0.01 e were considered as zero [41]. Negative electron populations coming from Mulliken Population Analysis were

corrected as usual [55]. Since the resolution of the system of linear equations is not possible because we have not enough molecules, we made use of Linear Multiple Regression Analysis (LMRA) techniques to find the best solution. For each case, a matrix containing the dependent variable (the inhibitory activity of each case) and the local atomic reactivity indices of all atoms of the common skeleton as independent variables was built. The Statistica software was used for LMRA [56]. We worked with the *common skeleton hypothesis* stating that there is a definite collection of atoms, common to all molecules analyzed, that accounts for nearly all the biological activity. The action of the substituents consists in modifying the electronic structure of the common skeleton and influencing the right alignment of the drug throughout the orientational parameters. It is hypothesized that different parts or this common skeleton accounts for almost all the interactions leading to the expression of a given biological activity. The common skeleton for the urea-based derivatives is shown in Fig. 2.

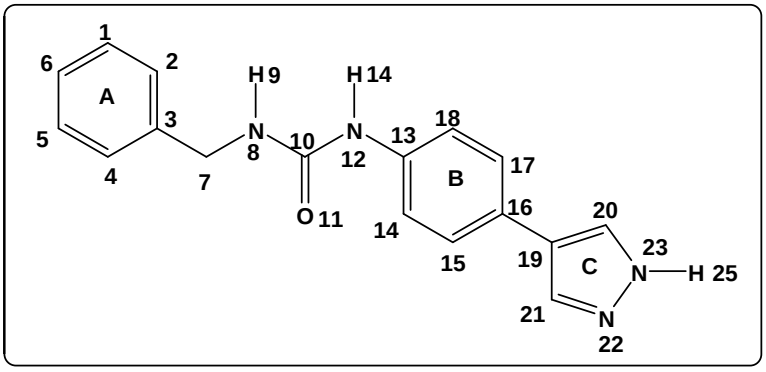

Figure 2. Common skeleton of urea-based molecules

RESULTS

Results for PKA inhibition

No statistically significant equation was obtained for n=20. As no outlier were found, we extracted the highest log(IC_{50}) value from the set and searched for a statistically significant equation. This procedure was followed until obtaining the following equation:

$$\log(IC_{50}) = 4.53 - 2.90F_{10}(\mathrm{LUMO}+2)^* - 2.15F_{17}(\mathrm{HOMO}-2)^* - 0.05S_{24}^{N}(\mathrm{LUMO})^* - \\ -9.78F_{19}(\mathrm{LUMO}+1)^* + 0.14\mu_9 \quad (1)$$

with n=17, R=0.96, R^2=0.93, adj-R^2=0.90, F(5,11)=29.48 (p<0.00001) and SD=0.18. No outliers were detected and no residuals fall outside the ±2σ limits. Here, F_{10}(LUMO+2)* is the Fukui index of the third lowest vacant MO localized on atom 10, F_{17}(HOMO-2)* is the Fukui index of the third highest occupied MO localized on atom 17, S_{24}^{N}(LUMO)* is the nucleophilic superdelocalizability of the lowest vacant MO localized on atom 24, F_{19}(LUMO+1)* is the Fukui index of the second lowest vacant MO localized on atom 19 and μ_9 is the local electronic chemical potential of atom 9. Tables 2 and 3 show the beta coefficients, the results of the t-test for significance of coefficients and the matrix of squared correlation coefficients for the variables of Eq. 1. There are no significant internal correlations between independent variables (Table 3). Figure 3 displays the plot of observed *vs.* calculated log(IC_{50}).

Table 2. Beta coefficients and t-test for significance of coefficients in Eq. 1

Var.	Beta	B	t(11)	*p*-level
F_{10}(LUMO+2)*	-0.95	-2.90	-8.10	<0.000006
F_{17}(HOMO-2)*	-0.56	-2.15	-4.73	<0.0006
S_{24}^{N}(LUMO)*	-0.51	-0.05	-5.27	<0.0003
F_{19}(LUMO+1)*	-0.35	-9.78	-4.27	<0.001
μ_9	0.26	0.14	2.55	<0.03

Table 3. Matrix of squared correlation coefficients for the variables in Eq. 1

	F_{10}(LUMO+2)*	F_{17}(HOMO-2)*	S_{24}^N(LUMO)*	F_{19}(LUMO+1)*
F_{10}(LUMO+2)*	1.00			
F_{17}(HOMO-2)*	0.18	1.00		
S_{24}^N(LUMO)*	0.07	0.11	1.00	
F_{19}(LUMO+1)*	0.00	0.03	0.01	1.00
μ_9	0.11	0.00	0.06	0.02

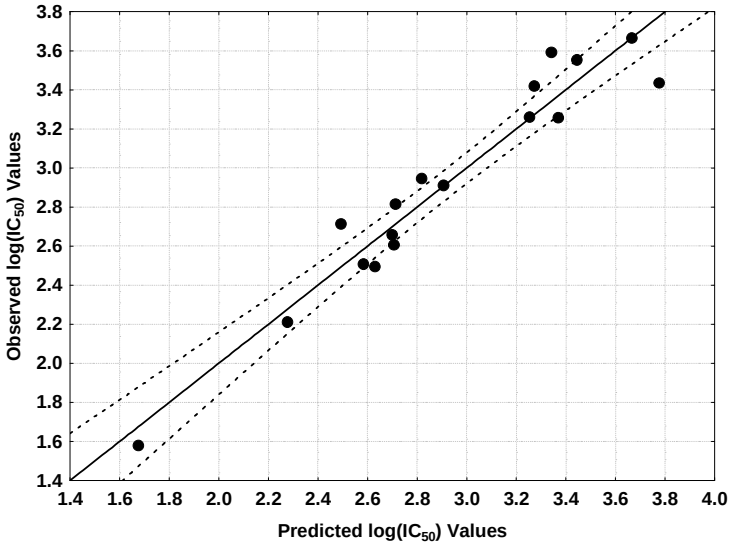

Figure 3. Plot of predicted *vs*. observed log(IC_{50}) values (Eq. 1). Dashed lines denote the 95% confidence interval.

The associated statistical parameters of Eq. 1 indicate that this equation is statistically significant and that the variation of the numerical values of a group of five local atomic reactivity indices of atoms of the common skeleton explains about 90% of the variation of log(IC_{50}) in this group of urea-based derivatives. Figure 3, spanning about 2.2 orders of magnitude, shows that there is a good correlation of observed *versus* calculated values and that almost all points are inside the 95% confidence interval. This can be considered as an indirect evidence that the common skeleton hypothesis works relatively well for this set of molecules. A very important point to stress is the following. When a local atomic reactivity index of an inner occupied MO (i.e., HOMO-1 and/or HOMO-2) or of a higher vacant MO (LUMO+1 and/or LUMO+2) appears in any equation, this means that the remaining of the upper occupied MOs (for example, if HOMO-2 appears, upper means HOMO-1 and HOMO) or the remaining of the empty MOs (for example, if LUMO+1 appears, lower means the LUMO) contribute to the interaction. Their absence in the equation only means that the variation of their numerical values does not account for the variation of the numerical value of the biological property.

Results for ROCK2 inhibition

The best equation obtained was:

$$\log(IC_{50}) = 4.48 - 4.04F_3(\text{LUMO})^* - 23.91F_{19}(\text{LUMO})^* - \\ -0.02S_{13}^N(\text{LUMO})^* + 0.003S_{17}^N(\text{LUMO}+2)^* \quad (2)$$

with n=17, R=0.99, R^2=0.98, adj-R^2=0.98, F(4,12)=179.99 (p<0.000001) and SD=0.16. No outliers were detected and no residuals fall outside the ±2σ limits. Here, F_3(LUMO)* is the Fukui index of the lowest vacant MO localized on atom 3, F_{19}(LUMO)* is the Fukui index of the lowest vacant MO localized on atom 19, S_{13}^N(LUMO)* is the nucleophilic superdelocalizability of the lowest vacant MO localized on atom 13 and S_{17}^N(LUMO+2)* is the nucleophilic superdelocalizability of the third lowest vacant MO localized on atom 17. Tables 4 and 5 show the beta coefficients, the results of the t-test for significance of coefficients and the matrix of squared correlation coefficients

for the variables of Eq. 2. There are no significant internal correlations between independent variables (Table 5). Figure 4 displays the plot of observed *vs.* calculated log(IC_{50}).

Table 4. Beta coefficients and t-test for significance of coefficients in Eq. 2

Var.	Beta	t(12)	*p*-level
F_3(LUMO)*	-0.72	-19.17	<0.000001
F_{19}(LUMO)*	-0.59	-15.58	<0.000001
S_{13}^N(LUMO)*	-0.29	-7.64	<0.000006
S_{17}^N(LUMO+2)*	0.25	6.55	<0.00003

Table 5. Matrix of squared correlation coefficients for the variables in Eq. 2

	F_3(LUMO)*	F_{19}(LUMO)*	S_{13}^N(LUMO)*
F_3(LUMO)*	1.00		
F_{19}(LUMO)*	0.003	1.00	
S_{13}^N(LUMO)*	0.01	0.04	1.00
S_{17}^N(LUMO+2)*	0.01	0.01	0.02

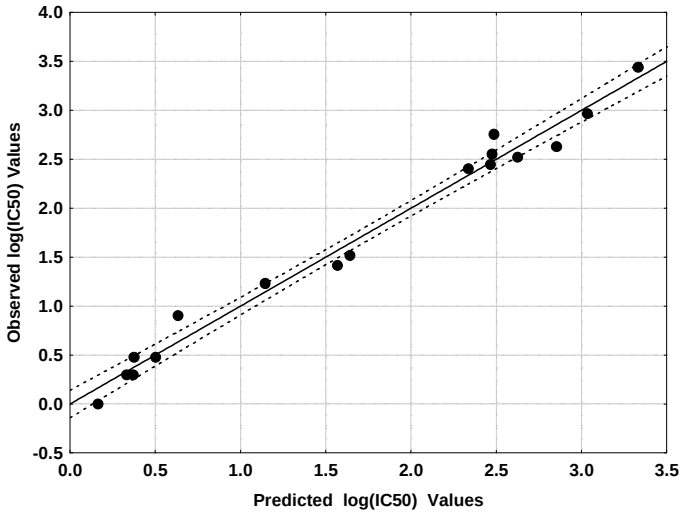

Figure 4. Plot of predicted *vs*. observed log(IC_{50}) values (Eq. 2). Dashed lines denote the 95% confidence interval.

The associated statistical parameters of Eq. 2 indicate that this equation is statistically significant and that the variation of the numerical values of a group of four local atomic reactivity indices of atoms of the common skeleton explains about 98% of the variation of log(IC_{50}) in this group of urea-based derivatives. Figure 4, spanning about 3 orders of magnitude, shows that there is a good correlation of observed *versus* calculated values and that almost all points are inside the 95% confidence interval. This can be considered as an indirect evidence that the common skeleton hypothesis works relatively well for this set of molecules.

Local Molecular Orbitals

Tables 6 to 8 shows the local MO structure of atoms 3, 9, 10, 13, 17, 19 and 24 (see Fig. 2). Nomenclature: Molecule (HOMO) / (HOMO-2)* (HOMO-1)* (HOMO)* - (LUMO)* (LUMO+1)* (LUMO+2)*.

Table 6. Local molecular orbital structure of atoms 3, 9 and 10

Mol.	Atom 3 (C)	Atom 9 (H or C)	Atom 10 (C)
1 (85)	80π83π84π-86π88π91σ	62σ65σ67σ-94σ95σ97σ	83σ84σ85π-86σ87π90π
2 (85)	82σ83σ84π-86σ87π88π	60σ65σ67σ-91σ92σ93σ	83σ84σ85σ-87π88σ90π
3 (81)	78π79π80π-82π83π84π	64σ65σ75σ-83σ87σ89σ	77σ79σ80σ-82σ83σ87σ
4 (81)	78σ79π81π-83π84π85π	63σ64σ68σ-83σ85σ87σ	78π79σ80σ-82π87π88π
5 (85)	82π83π84π-86π87π91σ	63σ64σ71σ-91σ92σ93σ	83π84σ85σ-88π92π93π
6 (81)	74π75π80π-82π83π87σ	60σ64σ68σ-87σ91σ92σ	79π80σ81σ-84π88π89π
7 (89)	83π87π88π-90π91π93π	70σ75σ86σ-95σ97σ99σ	86σ87σ89π-90π91π92π
8 (97)	93π94π95π-98π99π101π	67σ77σ78σ-103σ105σ106σ	92σ93σ94σ-98π103σ106π
9 (93)	88π89π92π-94π95π96π	68σ70σ76σ-101σ102σ104σ	91π92σ93σ-94π95σ99π
10 (93)	89π90π91π-94π95π96π	66σ71σ74σ-99σ103σ104σ	88π90π92σ-94π98π99σ
11 (89)	84π86π88π-90π91π93π	71σ76σ87σ-95σ96σ99σ	84π86π87σ-90π94π96σ
12 (109)	104π106π107π-110π111π112π	76σ80σ89σ-117σ118σ120σ	106σ107σ108σ-110σ111σ115π
13 (116)	80π83π84π- 86π88π91σ	76σ86σ93σ-124σ125σ128σ	113σ114σ115σ-118σ122π124σ
14 (113)	82σ83σ84π-86σ87π88π	90σ105σ109σ-119σ120σ121σ	83σ84σ85π-86σ87π90π
15 (113)	78π79π80π-82π83π84π	108σ109σ111σ -122σ123σ126σ	83σ84σ85σ-87π88σ90π
16 (117)	78σ79π81π-83π84π85π	102σ112σ113σ-124σ127σ129σ	77σ79σ80σ-82σ83σ87σ
17 (85)	82π83π84π-86π87π89π	61σ64σ68σ-93σ94σ95σ	78π79σ80σ-82π87π88π
18 (93)	88π89π92π-94π95π96σ	62σ69σ74σ-99σ101σ102σ	83π84σ85σ-88π92π93π
19 (93)	89π91π92π-95π96π97π	74σ76σ91σ-97σ99σ102σ	79π80σ81σ-84π88π89π
20 (93)	91π92π93π-94π95π97π	75σ77σ90σ-99σ101σ102σ	86σ87σ89π-90π91π92π
21 (93)	88π89π92π-94π95π97σ	64σ69σ74σ-99σ101σ102σ	92σ93σ94σ-98π103σ106π
22 (93)	89π91π92π-94π95π97π	73σ77σ90σ-99σ100σ103σ	90σ91σ93σ-94π98π100σ
23 (93)	89π91π92π-94π95π96π	68σ70σ74σ-101σ102σ103σ	90σ91σ93σ-94π95σ99π
24 (89)	85π86π88π-90π91π92π	66σ69σ70σ-95σ99σ100σ	87σ88σ89σ- 91σ92σ96π
25 (89)	84π87π88π-90π91π93π	82σ86σ88σ-99σ104σ106σ	80π86σ88σ-91π94π95σ

Table 7. Local molecular orbital structure of atoms 13, 17 and 19

Mol.	Atom 13 (C)	Atom 17 (C)	Atom 19 (C)
1 (85)	76π81π85π-87π88π89π	83π84π85π-87π89π90π	79π81π85π-87π90π92π
2 (85)	78π79π85π-87π88π89π	82π83π85π-87π88π89π	82π83π85π-87π90π91π
3 (81)	72π76σ81π-82π83π85π	78π80π81π-82π83π85π	76π77π81π-82π83π86π
4 (81)	72π75σ80π-82π84π86π	77π79π80π-82π84π85π	75π79π80π-82π86σ90π
5 (85)	76π80σ85π-86π88π89π	82π84π85π-88π89π90π	83π84π85π-88π90π93π
6 (81)	72π77σ81π-84π85π86π	79π80π81π-84π85π86π	77π79π81π-84π86π88π
7 (89)	82π83π89π-90π91π92π	85π87π89π-91π92π96π	84π85π89π-91π94π96π
8 (97)	92σ96π97π-98π99π100π	92π96π97π-98π99π100π	92π96π97π-98π102π103π
9 (93)	84π88σ93π-94π95π97π	91π92π93π-94π95π97π	90π91π93π-94π95π97π
10 (93)	86π89π93π-94π95σ96π	89π90π93π-94π95π96π	89π90π93π-94π96π98π
11 (89)	82π85π89π-90π91π92π	83π85π89π-90π91π92π	85π86π89π-90π91π94π
12 (109)	99π103π108π-110π111π113π	105π106π107π-111π113π114π	106π107π108π-111π113π114π
13 (116)	110π115π116π-117π118π120π	114π115π116π-117π118π120π	112π113π115π-118π120π121π
14 (113)	111π112π113π-114π116π118π	111π112σ113π-114π116π118π	107π111π112π-114π118π119π
15 (113)	76π81π85π-87π88π89π	83π84π85π-87π89π90π	107π110π112π-114π117π118π
16 (117)	78π79π85π-87π88π89π	82π83π85π-87π88π89π	79π81π85π-87π90π92π
17 (85)	72π76σ81π-82π83π85π	78π80π81π-82π83π85π	82π83π85π-87π90π91π
18 (93)	83π87σ93π-94π95π96π	77π79π80π-82π84π85π	76π77π81π-82π83π86π
19 (93)	84π87σ93π-94π95π96π	89π91π93π-94π95π96π	75π79π80π-82π86σ90π
20 (93)	86π92π93π-94π95π96π	91π92π93π-94π96π97π	83π84π85π-88π90π93π
21 (93)	84π87σ93π-94π95π96π	89π92π93π-94π95π96π	77π79π81π-84π86π88π
22 (93)	84π86π93π-94π95π96π	88π89π93π-94π96π98π	87π88π93π-94π95π96π
23 (93)	84π87σ93π-94π96π98π	90π91π93π-94π96π98π	87π90π93π-94π98π99π
24 (89)	80π84σ89π-91π92π93π	86π88π89π-91π92π93π	84π87π89π-91π92π94π
25 (89)	80π85π89π-90π91π92π	83π85π89π-91π92π94π	83π84π89π-91π94π96π

Table 8. Local molecular orbital structure of atom 24

Mol.	Atom 24 (H)		Mol.	Atom 24 (H)
1 (85)	67σ71σ8 σ-91σ92σ97σ		14 (113)	95σ102σ109σ-114σ118σ119σ
2 (85)	56σ65σ66σ-86σ87σ88σ		15 (113)	94σ103σ108σ-114σ116σ119σ
3 (81)	67σ72σ80σ-82σ83σ85σ		16 (117)	98σ106σ112σ-118σ123σ125σ
4 (81)	67σ72σ79σ-82σ84σ85σ		17 (85)	71σ76σ83σ-86σ87σ90σ
5 (85)	72σ76σ84σ-86σ87σ89σ		18 (93)	78σ83σ92σ-94σ95σ98σ
6 (81)	69σ72σ80σ-84σ85σ87σ		19 (93)	74σ77σ84σ-94σ98σ99σ
7 (89)	70σ76σ86σ-95σ99σ103σ		20 (93)	75σ78σ90σ-99σ101σ102σ
8 (97)	82σ87σ94σ-98σ100σ103σ		21 (93)	78σ84σ92σ-94σ96σ99σ
9 (93)	76σ77σ84σ-94σ99σ100σ		22 (93)	75σ78σ90σ-99σ103σ106σ
10 (93)	60σ74σ92σ-99σ100σ102σ		23 (93)	78σ84σ91σ-94σ96σ99σ
11 (89)	71σ74σ87σ-95σ96σ98σ		24 (89)	75σ80σ88σ-91σ93σ96σ
12 (109)	89σ91σ99σ-111σ117σ118σ		25 (89)	72σ75σ86σ-95σ98σ99σ
13 (116)	93σ94σ106σ-117σ118σ122σ			

DISCUSSION

Discussion of PKA inhibition

Table 2 shows that the importance of variables in Eq. 1 is F_{10}(LUMO+2)*>> F_{17}(HOMO-2)*> S_{24}^{N}(LUMO)*> F_{19}(LUMO+1)*> μ_9. A high PKA inhibition is associated with large values for F_{10}(LUMO+2)*, F_{17}(HOMO-2)* and F_{19}(LUMO+1)*. If S_{24}^{N}(LUMO)* is positive, a high inhibitory activity is associated with large numerical values for this index. Since μ_9 is negative, a high inhibitory activity is associated with large (negative) values for this local reactivity index. Atom 10 is the carbon atom of the C_{10}=O_{11} moiety in the chain linking rings A and B (Fig. 2). A high value for F_{10}(LUMO+2)* suggests that this atom is interacting with an occupied MO. Table 6 shows that $(LUMO+2)_{10}^{*}$ has, at the level of the approximations used in the model, σ or π natures. Therefore, the best condition for an optimal inhibitory activity is that the three lowest vacant MOs have a π nature. Atom 17 is a carbon atom in ring B (Fig. 2). A high value for F_{17}(HOMO-2)* suggests that this atom is interacting with a vacant MO. Table 7 shows that the three highest occupied local MOs have a π nature in all molecules, reinforcing the idea that an optimal inhibitory activity seems to be associated with the interaction of these three MOs with one or more vacant MOs. Atom 24 is the atom attached to N-12 in the chain linking rings A and B (Fig. 2). $(LUMO)_{24}^{*}$ is a σ MO (Table 8). Large positive values for S_{24}^{N}(LUMO)* are obtained by shifting downwards the associated eigenvalue, making this MO more reactive. This suggests that atom 24 is acting as an electron-acceptor. Considering that this atom is hydrogen or carbon we could be in presence of an H-bond in the case of H atom. The exact role of a C atom is not clear, but it could be involved in a C-H…C interaction. Atom 19 is a carbon atom in ring C (Fig. 2). A high inhibitory activity is associated with large values for F_{19}(LUMO+1)*. As almost all the first two lowest vacant MOs have a π nature (Table 7), we suggest that atom 19 in interacting with an electron-rich center. Atom 9 is the atom bonded to N-8 in the chain linking rings A and B (H or C, Fig. 2). All MOs have a σ nature (Table 6). A high inhibitory activity is associated with large (negative) values for μ_9. This index corresponds to the midpoint of the $(HOMO)_{19}^{*}$ and $(LUMO)_{19}^{*}$ energies. These two MOs have a π nature. From a strict theoretical point of view, there are three ways to obtain more negative values for μ are shown in Fig. 5.

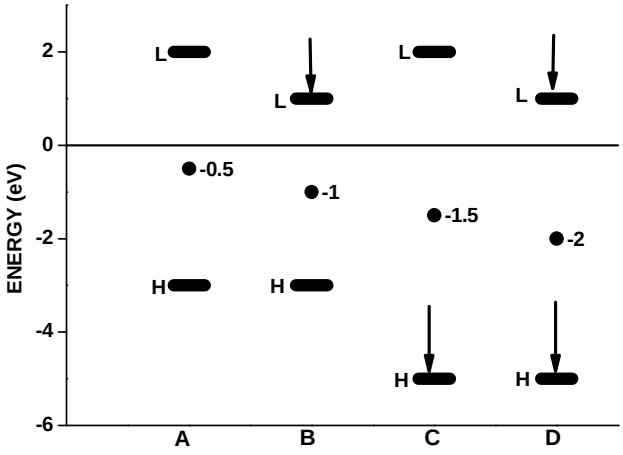

Figure 5. Modification of the value of the local atomic electronic chemical potential. H stands for HOMO and L for LUMO, black dots denote the local μ position and value. Arrows indicate what eigenvalue was shifted downwards

In this figure A denotes the original case: local μ is located at -0.5 eV. In case B we have shifted downwards the LUMO energy and μ has now a value of -1 eV. In case C the HOMO energy was shifted downwards and μ has a value of -1.5. In case D we shifted downwards simultaneously the energy of both local frontier MOs and the μ value moves to -2 eV. Note that in the last case the magnitude of both shifting does not to be the same. Now, and from a practical point of view, the easiest way to obtain a larger negative value for μ is for case B. This is so because, if the electronic distribution and energies of the inner occupied local molecular orbitals are not modified, repulsive interactions among occupied (local) MOs will intensify. We can imagine this situation by using an extremely simple picture in which the occupied MO are envisaged as the layers of a multilayer sandwich: if we pushed below the upper layer the ones lying below will be compressed and, at the end, they will mix. This situation becomes clearer when we have the case of an atom in which the local HOMO is located energetically very far from the molecule's HOMO. Within this reasoning, we suggest that the inhibitory activity will raise when the local LUMO becomes more reactive (case B of Fig. 5). Therefore, atom 19 is interacting with an electron-rich center. This is consistent with the formation of a N_8-H_9…X hydrogen bond. All the suggestions are displayed in the partial 2D pharmacophore of Fig. 6.

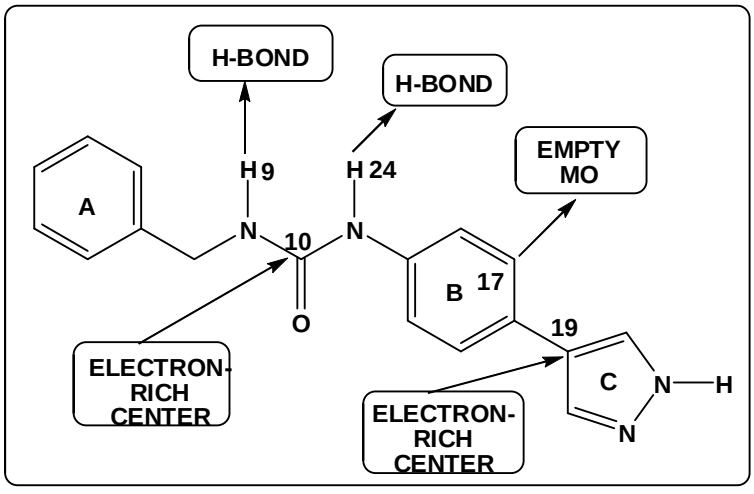

Figure 6. 2D pharmacophore for PKA inhibition by urea-based molecules

DISCUSSION

Table 4 shows that the importance of variables in Eq. 2 is F_3(LUMO)*> F_{19}(LUMO)*>> S_{13}^N(LUMO)*> S_{17}^N(LUMO+2)*. A high ROCK2 inhibition is associated with large values for F_3(LUMO)* and F_{19}(LUMO)*. If S_{13}^N(LUMO)* is positive, a good inhibitory capacity is associated with a large numerical value for this reactivity index. If S_{17}^N(LUMO+2)* is positive, a good inhibitory activity is associated with a small numerical value for this index. Atom 3 is a carbon atom in ring A (Fig. 2). A high inhibitory activity is associated with a large value for F_3(LUMO)*. This MO has a π nature in almost all molecules (Table 6). Therefore, atom 3 seems to interact with an electron-rich center. Atom 19 is a carbon atom in ring C (Fig. 2). A high inhibitory activity is associated with a large value for F_{19}(LUMO)*. Table 7 indicates that this MO has a π nature in all molecules. This allows to suggest that atom 19 is interacting with an electron-rich center. Atom 13 is a carbon atom in ring B (Fig. 2). A high inhibitory activity is associated with a large numerical value of S_{13}^N(LUMO)* if the numerical value for this reactivity index is positive. If negative, a high inhibitory activity is associated with a small negative numerical value. We consider both possibilities because it is well known that many results of quantum chemical calculations (at the *ab initio* and DFT levels) report vacant MOs with negative energies. Figure 7 explains how to increase or diminish S^N and S^E values.

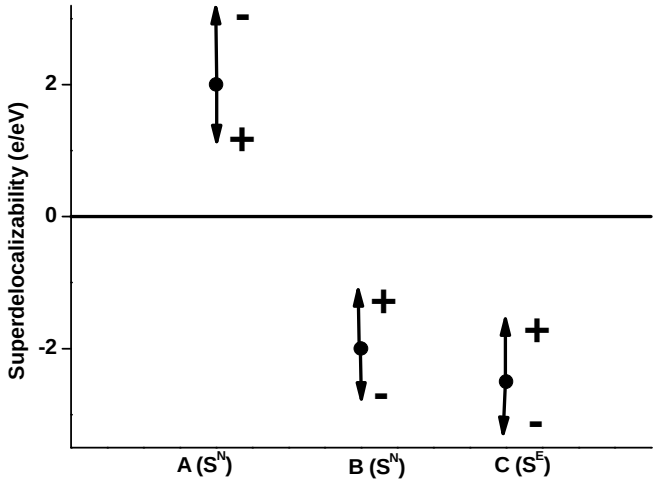

Figure 7. How to obtain higher or lower numerical values for nucleophilic and electrophilic superdelocalizabilities associated with only one MO

A positive S^N value is shown in A of Fig. 7. To obtain greater numerical values for this index we can shift downwards the energy of the associated eigenvalue (+). This is so because the MO energy is in the denominator of the expression defining the superdelocalizabilities. To obtain smaller values, we shift upwards the energy of the associated eigenvalue (-). B shows the case of a negative numerical value of S^N. Now, if we need to get larger negative values we need to shift upwards the energy of the associated eigenvalue (+). Shifting downwards the value of the associated eigenvalue will produce smaller negative values (-). Case C refers to electrophilic superdelocalizabilities. As they are always negative in closed shell systems, we work with them as in case B. In the case of atom 13 we can see that a large positive numerical value or a small negative numerical value are associated with a high inhibitory activity. Fig. 7 shows that in both situations the associated LUMO energy must be shifted downwards making the MO more reactive. Therefore, we suggest that atom 13 is interacting with an electron-rich moiety. Atom 17 is a carbon atom in ring B (Fig. 2). A high inhibitory activity is associated with a small numerical value of S_{17}^N(LUMO+2)* if the value of this index is positive. Fig. 7 shows that this MO should be made less reactive. This could be a possible signal of a repulsive interaction of this MO with vacant MOs of the partner. Unhappily, Eq. 2 is not able to show the role of $(LUMO+1)_{17}^*$ and $(LUMO)_{17}^*$. Plots of the numerical values of S_{17}^N(LUMO+1)* and S_{17}^N(LUMO)* *vs.* log(IC_{50}) (not shown here) show that, in general, the inhibitory activity increases when these two MOs become lees reactive. Therefore we suggest that atom 17 is interacting with an

electron-deficient center. This suggestion is provisory. All the suggestions are displayed in the partial 2D pharmacophore shown in Fig. 8.

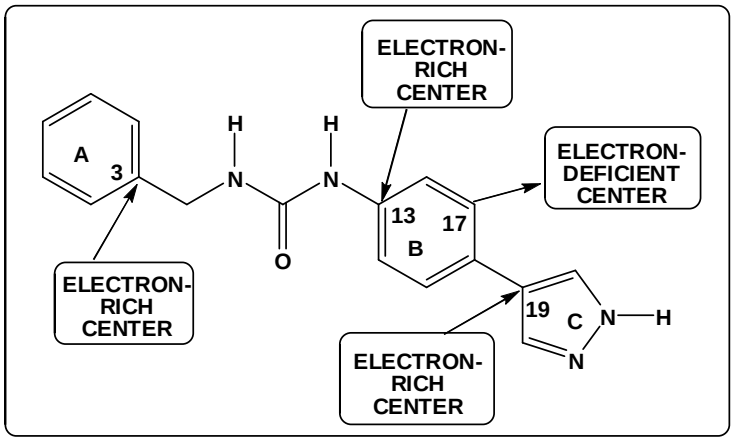

Figure 8. 2D pharmacophore for ROCK2 inhibition by urea-based molecules

In conclusion, we obtained statistically significant equations relating the variation of the PKA and ROCK2 inhibitory potencies with the variation of the numerical values of definite sets of local atomic reactivity indices for a group of urea-based molecules. It is interesting to note the participation of two H-bonds of the urea moiety in the inhibition of PKA. Our intensive search for a biological activity that *cannot* be analyzed with the KPG method has proved to be unproductive up today [57].

REFERENCES

[1] D Mei, Y Yin, F Wu, J Cui, H Zhou, et al., *Biorg. Med. Chem.*, **2015**, 23, 2505-2517.
[2] C-H Weng, S Gupta, P Geraghty, R Foronjy, AB Pernis, *Mol. Immunol.*, **2016**, 71, 115-122.
[3] Y-C Liao, P-Y Liu, H-F Lin, W-Y Lin, JK Liao, et al., *J. Mol. Cell. Cardiol.*, **2015**, 79, 180-186.
[4] M Li, W Zhou, R Yuan, L Chen, T Liu, et al., *FEBS Lett.*, **2015**, 589, 1018-1025.
[5] EG Gentry, BW Henderson, M Gearing, Y Feng, JH Herskowitz, *Alz. Dement.*, **2015**, 11, P203.
[6] S Li, C Wang, Y Dai, Y Yang, H Pan, et al., *Tiss. Cell*, **2013**, 45, 387-396.
[7] HG Jin, H Yamashita, Y Nagano, H Fukuba, M Hiji, et al., *Neurosci. Lett.*, **2006**, 408, 62-67.
[8] S Shah, J Savjani, *Biorg. Med. Chem. Lett.*, **2016**, 26, 2383-2391.
[9] Y Xin, J Yu, C Liu, Y Li, L Feng, et al., *J. Neurol. Sci.*, **2015**, 357, Supplement 1, e322.
[10] BA Harrison, ZY Almstead, H Burgoon, M Gardyan, NC Goodwin, et al., *ACS Med. Chem. Lett.*, **2015**, 6, 84-88.
[11] D Shaw, G Hollingworth, N Soldermann, E Sprague, W Schuler, et al., *Biorg. Med. Chem. Lett.*, **2014**, 24, 4812-4817.
[12] VP Kale, JA Hengst, DH Desai, TE Dick, KN Choe, et al., *Canc. Lett.*, **2014**, 354, 299-310.
[13] P Pan, M Shen, H Yu, Y Li, D Li, et al., *Drug Discov. Tod.*, **2013**, 18, 1323-1333.
[14] S Chowdhury, YT Chen, X Fang, W Grant, J Pocas, et al., *Biorg. Med. Chem. Lett.*, **2013**, 23, 1592-1599.
[15] S Boland, O Defert, J Alen, A Bourin, K Castermans, et al., *Biorg. Med. Chem. Lett.*, **2013**, 23, 6442-6446.
[16] R Xu, A Banka, JF Blake, IS Mitchell, EM Wallace, et al., *Biorg. Med. Chem. Lett.*, **2011**, 21, 2335-2340.
[17] C-C Tsai, H-F Liu, K-C Hsu, J-M Yang, C Chen, et al., *Biochem. Pharmacol.*, **2011**, 81, 856-865.
[18] EH Sessions, S Chowdhury, Y Yin, JR Pocas, W Grant, et al., *Biorg. Med. Chem. Lett.*, **2011**, 21, 7113-7118.
[19] P Ray, J Wright, J Adam, S Boucharens, D Black, et al., *Biorg. Med. Chem. Lett.*, **2011**, 21, 1084-1088.
[20] P Ray, J Wright, J Adam, J Bennett, S Boucharens, et al., *Biorg. Med. Chem. Lett.*, **2011**, 21, 97-101.
[21] S Chowdhury, EH Sessions, JR Pocas, W Grant, T Schröter, et al., *Biorg. Med. Chem. Lett.*, **2011**, 21, 7107-7112.
[22] Y Yin, L Lin, C Ruiz, MD Cameron, J Pocas, et al., *Biorg. Med. Chem. Lett.*, **2009**, 19, 6686-6690.
[23] H Sagawa, H Terasaki, M Nakamura, M Ichikawa, T Yata, et al., *Exp. Neurol.*, **2007**, 205, 230-240.
[24] N Palacios, F Sánchez-Franco, M Fernández, I Sánchez, G Villuendas, et al., *Brain Res.*, **2007**, 1178, 1-11.
[25] TG Davies, ML Verdonk, B Graham, S Saalau-Bethell, CCF Hamlett, et al., *J. Mol. Biol.*, **2007**, 367, 882-894.

[26] H Reuveni, N Livnah, T Geiger, S Klein, O Ohne, et al., *Biochem.*, **2002**, 41, 10304-10314.
[27] Note. The results presented here are obtained from what is now a routinary procedure. For this reason, we built a general model for the paper's structure. This model contains *standard* phrases for the presentation of the methods, calculations and results because they do not need to be rewritten repeatedly.
[28] YC Martin, *Quantitative drug design: a critical introduction*, M. Dekker, New York, **1978**.
[29] JS Gómez-Jeria, *Elements of Molecular Electronic Pharmacology (in Spanish)*, Ediciones Sokar, Santiago de Chile, **2013**.
[30] F Peradejordi, AN Martin, A Cammarata, *J. Pharm. Sci*., **1971**, 60, 576-582.
[31] JS Gómez-Jeria, *Int. J. Quant. Chem.*, **1983**, 23, 1969-1972.
[32] F Tomas, JM Aulló, *J. Pharm. Sci*., **1979**, 68, 772-776.
[33] JS Gómez-Jeria, L Espinoza, *Bol. Soc. Chil. Quím.*, **1982**, 27, 142-144.
[34] JS Gómez-Jeria, D Morales-Lagos, "The mode of binding of phenylalkylamines to the Serotonergic Receptor," in *QSAR in design of Bioactive Drugs*, M. Kuchar Ed., pp. 145-173, Prous, J.R., Barcelona, Spain, **1984**.
[35] JS Gómez-Jeria, DR Morales-Lagos, *J. Pharm. Sci.*, **1984**, 73, 1725-1728.
[36] JS Gómez-Jeria, D Morales-Lagos, JI Rodriguez-Gatica, JC Saavedra-Aguilar, *Int. J. Quant. Chem.*, **1985**, 28, 421-428.
[37] JS Gómez-Jeria, D Morales-Lagos, BK Cassels, JC Saavedra-Aguilar, *Quant. Struct.-Relat.*, **1986**, 5, 153-157.
[38] JS Gómez-Jeria, BK Cassels, JC Saavedra-Aguilar, *Eur. J. Med. Chem.*, **1987**, 22, 433-437.
[39] JS Gómez-Jeria, "Modeling the Drug-Receptor Interaction in Quantum Pharmacology," in *Molecules in Physics, Chemistry, and Biology*, J. Maruani Ed., vol. 4, pp. 215-231, Springer Netherlands, **1989**.
[40] JS Gómez-Jeria, M Ojeda-Vergara, *J. Chil. Chem. Soc*., **2003**, 48, 119-124.
[41] JS Gómez-Jeria, *Canad. Chem. Trans.*, **2013**, 1, 25-55.
[42] JS Gómez-Jeria, M Flores-Catalán, *Canad. Chem. Trans*., **2013**, 1, 215-237.
[43] A Paz de la Vega, DA Alarcón, JS Gómez-Jeria, *J. Chil. Chem. Soc*., **2013**, 58, 1842-1851.
[44] I Reyes-Díaz, JS Gómez-Jeria, *J. Comput. Methods Drug Des.*, **2013**, 3, 11-21.
[45] F Gatica-Díaz, JS Gómez-Jeria, *J. Comput. Methods Drug Des.*, **2014**, 4, 79-120.
[46] J Valdebenito-Gamboa, JS Gómez-Jeria, *Der Pharma Chem.*, **2015**, 7, 543-555.
[47] HR Bravo, BE Weiss-López, J Valdebenito-Gamboa, JS Gómez-Jeria, *Res. J. Pharmac. Biol. Chem. Sci.*, **2016**, 7, 792-798.
[48] JS Gómez-Jeria, S Abarca-Martínez, *Der Pharma Chem.*, **2016**, 8, 507-526.
[49] JS Gómez-Jeria, R Cornejo-Martínez, *Der Pharma Chem.*, **2016**, 8, 329-337.
[50] JS Gómez-Jeria, C Moreno-Rojas, *Der Pharma Chem.*, **2016**, 8, 475-482.
[51] JS Gómez-Jeria, Í Orellana, *Der Pharma Chem.*, **2016**, 8, 476-487.
[52] A Robles-Navarro, JS Gómez-Jeria, *Der Pharma Chem.*, **2016**, 8, 417-440.
[53] MJ Frisch, GW Trucks, HB Schlegel, GE Scuseria, MA Robb, et al., "G03 Rev. E.01," Gaussian, Pittsburgh, PA, USA, **2007**.
[54] JS Gómez-Jeria, "D-Cent-QSAR: A program to generate Local Atomic Reactivity Indices from Gaussian 03 log files. v. 1.0," Santiago, Chile, **2014**.
[55] JS Gómez-Jeria, *J. Chil. Chem. Soc*., **2009**, 54, 482-485.
[56] Statsoft, "Statistica v. 8.0," 2300 East 14 th St. Tulsa, OK 74104, USA, **1984-2007**.
[57] Note, *All papers of Gómez-Jeria can be found in https://www.researchgate.net/profile/Juan-Sebastian_Gomez-Jeria*,